Zoological Journal of the Linnean Society, 2020, **XX**, 1–14. With 3 figures.

Warning signals promote morphological diversification in fossorial uropeltid snakes (Squamata: Uropeltidae)

VIVEK PHILIP CYRIAC[1,*] and ULLASA KODANDARAMAIAH[1]

[1]*IISER-TVM Centre for Research and Education in Ecology and Evolution (ICREEE) and School of Biology, Indian Institute of Science Education and Research Thiruvananthapuram, Maruthamala P.O., Vithura, Thiruvananthapuram, 695551, India*

Received 26 November 2019; revised 17 March 2020; accepted for publication 8 May 2020

Many species possess warning colourations that signal unprofitability to predators. Warning colourations are also thought to provide prey with a 'predator-free space' and promote niche expansion. However, how such strategies release a species from environmental constraints and facilitate niche expansion is not clearly understood. Fossoriality in reptiles imposes several morphological limits on head and body size to facilitate burrowing underground, but many fossorial snakes live close to the surface and occasionally move above ground, exposing them to predators. In such cases, evolving antipredator defences that reduce predation on the surface could potentially relax the morphological constraints associated with fossoriality and promote morphological diversification. Fossorial uropeltid snakes possess varying degrees of conspicuous warning colourations that reduce avian predation when active above ground. We predicted that species with more conspicuous colourations will exhibit more robust body forms and show faster rates of morphological evolution because constraints imposed by fossoriality are relaxed. Using a comparative phylogenetic approach on the genus *Uropeltis*, we show that more conspicuous species tend to have more robust morphologies and have faster rates of head-shape evolution. Overall, we find that the evolution of warning colourations in *Uropeltis* can facilitate niche expansion by influencing rates of morphological diversification.

ADDITIONAL KEYWORDS: antipredatory strategies – conspicuous colourations – morphological evolution – niche expansion.

INTRODUCTION

Predation is one of the most profound biotic interactions that directly affects the survival of an individual (Gurevitch *et al.*, 2000), and prey animals have evolved multiple strategies to escape being eaten. Many species possess defences that make them unprofitable to predators and signal their unprofitability through conspicuous warning colours (Ruxton *et al.*, 2004; Mappes *et al.*, 2005). Warning signals enhance predator learning, allowing predators to selectively avoid such unprofitable prey in future encounters (Aronsson & Gamberale-Stille, 2012; Stevens & Ruxton, 2012). Apart from reducing predation risk, studies have also suggested that evolving conspicuous colours that signal unprofitability can reduce the constraints of crypsis and promote niche expansion (Merilaita & Tullberg, 2005; Speed *et al.*, 2010). Possessing such antipredatory defences can potentially provide prey with a 'predator-free space' to utilize other resources and opportunities (Speed *et al.*, 2010), and in turn lead to niche expansion and increased lineage diversification rate (Ehrlich & Raven, 1964; Przeczek *et al.*, 2008; Agrawal *et al.*, 2009; Weber & Agrawal, 2014; Arbuckle & Speed, 2015). We here test the hypothesis that the evolution of warning signals facilitates niche expansion in a group of fossorial snakes.

Fossorial (underground) environments are structurally simple and homogenous, and fossorial animals are generally considered to experience less predation compared to those living in above-ground environments (Nevo, 1979; Pipan *et al.*, 2010). The stability of fossorial environments forces fossorial species to become highly specialized in several aspects of their morphology, physiology, life history and behaviour (Nevo, 1979; see also: Cyriac

*Corresponding author. E-mail: vivek.philip14@iisertvm.ac.in

& Kodandaramaiah, 2018). Although fossoriality generally reduces exposure to predators (Nevo, 1979), moving underground is energetically expensive compared to moving on the surface (Navas *et al.*, 2004; Wu *et al.*, 2015) and thus imposes several morphological constraints on body size (Gans, 1960, 1968; Gans *et al.*, 1978; Nevo, 1979; Navas *et al.*, 2004). In head-first burrowing reptiles, it has been shown that energy constraints associated with a fossorial lifestyle limits the overall body size (Navas *et al.*, 2004; Camacho *et al.*, 2015; Wu *et al.*, 2015) and head shape (Navas *et al.*, 2004; Roscito & Rodrigues, 2010; Vanhooydonck *et al.*, 2010; Barros *et al.*, 2011; Hohl *et al.*, 2017), and these morphological features can determine the burrowing ability of a species (Navas *et al.*, 2004; Vanhooydonck *et al.*, 2010; Wu *et al.*, 2015; Hohl *et al.*, 2017). Theory and experiments have shown that relying on crypsis limits the habitats in which an animal can live (Merilaita *et al.*, 1999; Merilaita *et al.*, 2001; Merilaita & Lind, 2005; Bond & Kamil, 2006; Houston *et al.*, 2007). On the other hand, the evolution of secondary antipredatory defences would allow prey species to be more exposed, and thus reduce the constraints associated with a particular environment (Merilaita & Tullberg, 2005; Speed *et al.*, 2010). Many species of fossorial snakes also exhibit conspicuous body colouration (Greene, 1979, 1988), a trait that is unexpected in species living in environments devoid of light (Wollenberg & Measey, 2009). However, many species of fossorial reptiles can be found close to the surface for a relatively short period during the day or are active above the surface only during particular seasons (Gans, 1968; Cyriac & Kodandaramaiah, 2019a). Recent experiments on fossorial uropeltid snakes (family Uropeltidae) have shown that such conspicuous colours have an antipredatory function when they are exposed on the surface (Cyriac & Kodandaramaiah, 2019a). Evolving such antipredator defences, which reduce predation pressure when fossorial species are active on the surface, can potentially reduce the morphological constraints associated with fossoriality and promote niche expansion and morphological diversification.

To test if evolution of antipredator defences can facilitate morphological diversification in fossorial snakes, we focused on uropeltid snakes (family Uropeltidae), a group of fossorial snakes endemic to peninsular India and Sri Lanka, and exhibiting varying degree of bright, ventral colourations across species (Cyriac & Kodandaramaiah, 2019a). Although fossorial, these snakes are active above ground or near the surface during the monsoons, which exposes them to predators. Experiments have shown that the conspicuous colouration in these snakes reduces predation rates and functions as warning signals to advertise unprofitability associated with long handling times (Cyriac & Kodandaramaiah, 2019a, b). Apart from their colourations, uropeltid snakes also show variation in their body size and cranial morphology across species, associated with their fossorial habits (Rieppel, 1977; Rieppel & Zaher, 2002; Olori & Bell, 2012). Studies indicate that fossorial reptiles tend to have a narrow head with a thin and long body compared to their surface counterparts. These traits are thought to increase underground locomotor performance and help cope with the energetic demands of an underground lifestyle (Navas *et al.*, 2004; Camacho *et al.*, 2015; Wu *et al.*, 2015). Since conspicuous colouration in uropeltid snakes reduces predation when active above ground (Cyriac & Kodandaramaiah, 2019a), we expected species that exhibit more conspicuous colouration to be more active close to the surface and exhibit more robust body size associated with movement above ground. Additionally, evolving defences that reduce predation may allow fossorial species to occupy above-ground habitats (i.e. they are less bound to fossorial habitats), and because they are not constrained by fossoriality, their morphology can diversify faster or to a greater extent. We test these hypotheses using a comparative phylogenetic approach based on a multilocus phylogeny of the genus *Uropeltis*. We specifically test if the amount of conspicuous colouration in *Uropeltis* is positively correlated to body size, head morphology and rates of morphological evolution.

MATERIAL AND METHODS

Phylogenetic analysis and divergence dating

Sampling of *Uropeltis*, which is endemic to peninsular India, was carried out as part of another study between 2013 and 2015 within the state of Kerala, India. Collected samples were photographed, euthanized and preserved in ethanol, after which heart or liver tissue was collected for DNA extraction. DNA extraction and PCR amplification protocols follow Cyriac & Kodandaramaiah (2017). In addition to the four genes sequenced by Cyriac & Kodandaramaiah (2017), we sequenced the PRLR gene (prolactin receptor gene; Supporting Information, Table S1) for the *Uropeltis* species included in Cyriac & Kodandaramaiah (2017) and three additional species (see Supporting Information, Table S2). We sequenced both forward and reverse strands for the PRLR gene, manually checked for ambiguous sites and built a consensus sequence for each species using MEGA7 (Kumar *et al.*, 2016). For each gene alignment, we combined the additional sequences from Cyriac & Kodandaramaiah (2017) (Supporting Information, Table S2), realigned the sequences using the MUSCLE algorithm (Edgar, 2004) in MEGA7 and removed gaps using Gap Strip/squeeze v.2.1.0 (http://www.hiv.lanl.gov) with a 75% gap

tolerance. We concatenated the five-gene dataset using SequenceMatrix v.1.8 (Vaidya *et al.*, 2011). We divided the dataset into blocks based on codon position within each gene and used PartionFinder v.2.0.1 (Lanfear *et al.*, 2016) to find the best fit nucleotide substitution model and partition scheme (Supporting Information, Table S3). We used MrBayes 3.2.0 (Ronquist *et al.*, 2012) to infer phylogenetic relationships from the concatenated dataset using default priors. We implemented two independent Markov chain Monte Carlo (MCMC) runs for 8 million generations. We assumed convergence between the two independent MCMC runs by confirming that the average standard deviation of split frequencies fell below 0.01 and by examining the trace plots and posterior probability distribution using TRACER v.1.6 (Rambaut *et al.*, 2014). We also ensured there was appropriate mixing by confirming that the effective sample size (ESS) of each model parameter was greater than 200. We summarized the trees as a 50% majority rule tree after discarding 25% of the samples as burn-in.

Since there are no reliable fossil calibration points within Uropeltidae for the divergence dating analysis, we built a larger dataset with representative sequences for the five gene regions from major lineages within alethinophidian snakes (Alethinophidia) using sequence data from Genbank. In cases where there were multiple sequences of the same gene region for a species, we retained only one sequence per species. Since Uropeltidae is known to have high cryptic diversity (Cyriac & Kodandaramaiah, 2017), we included only sequences from operational taxonomic units (OTUs) that were identified by their morphological and/or phylogenetical distinctiveness based on the MrBayes topology. We partitioned the larger dataset into five bins as determined by TIGER v.1.0.2 (Cummins & McInerney, 2011) and used PartitionFinder to find the best-fit substitution model and partition scheme (Supporting Information, Table S3), after which we estimated the divergence times using BEAST 2.5.2 (Bouckaert *et al.*, 2014) in CIPRES Science Gateway v.3.3 (Miller *et al.*, 2010). We calibrated the tree by enforcing three topological constraints and four temporal constraints as in Cyriac & Kodandaramaiah (2017) (see Supporting Information, Table S4). We ran two independent analyses for 50 million generations using a relaxed uncorrelated log normal clock under the Yule speciation prior with other priors set to default values. We checked the two runs for convergence in TRACER v.1.6 by examining the ESS of the model parameters, and used LogCombiner v.2.3.0 and TreeAnnotator v.2.3.0 from the BEAST2 package to combine the two logs and eventually constructed a maximum clade credibility tree. We then pruned this tree to include just the 24 species of the genus *Uropeltis*.

Quantifying colouration

In order to quantify the overall proportion of conspicuous colouration, we compiled photographs of the dorsal and ventral sides of all 24 *Uropeltis* species represented in the tree. Photographs were obtained from our personal collection or taken from the *Reptiles of India v.1.22* web portal (Khandekar *et al.*, 2019) when the identity of the species was known. Photographs were also obtained from preserved specimens from our collection and from specimens of the Zoological Survey of India, Western Ghat Regional Centre (ZSI-WGRC). Although preserved specimens lose the yellow pigmented colouration in the preservative, we could still quantify the proportion of conspicuous colouration based on the discoloured patches that contrast from the background black or brown colouration (Supporting Information, Fig. S1). To quantify the relative amount of conspicuous colouration, we asked 45 volunteers to rate the proportion of conspicuous colours on the dorsal and ventral sides of each species. Since all the *Uropeltis* species included in the phylogenetic analyses had some degree of warning colours, we asked the volunteers to score colouration on a scale of 1–5 (1 being 1–20% conspicuously coloured and 5 being 81–100% conspicuously coloured). When photographs of multiple individuals of a species were available, we averaged the values for all individuals, to account for variation within species. We averaged all conspicuousness scores (CS) for the dorsal and ventral colouration and summed the scores to get the overall conspicuousness score (ΣCS_i) for each species. We also calculated the interclass correlation coefficient for the dorsal, ventral and overall conspicuousness scores to evaluate the inter-observer agreement for each species (for details, see Supporting Information, Table S5). The rounded off (to the nearest whole number) overall conspicuous scores ranged from 2 (least conspicuous) to 6 (most conspicuous). We then binarized the ΣCS_i values as being less conspicuous (state 0) or more conspicuous (state 1), using three threshold schemes to account for inter-individual variation (Fig. 1). The threshold values were of increasing ΣCS_i and were categorized under a liberal scheme where $\Sigma CS_i \geq 3$ was scored as 1, an intermediate scheme where $\Sigma CS_i \geq 4$ was scored as 1 and a strict scheme where $\Sigma CS_i \geq 5$ was scored as 1. We acknowledge that such a qualitative measure for conspicuousness based on human assessment of photographs may be prone to error. However, it should be noted that previous experiments suggest that uropeltid colouration is highly conspicuous to avian predators (Cyriac & Kodandaramaiah, 2019a), and that humans and birds see colour similarly, such that colours that are conspicuous to humans are also conspicuous to birds (Vorobyev *et al.*, 2001).

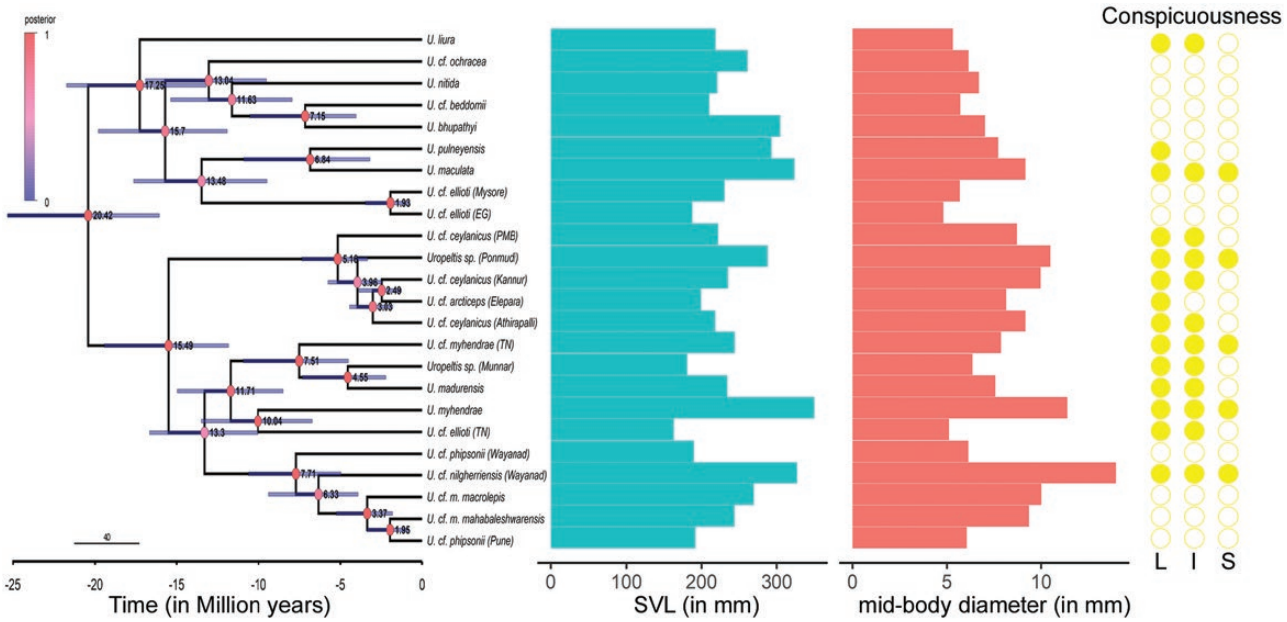

Figure 1. Maximum clade credibility tree of *Uropeltis* from the BEAST analysis along with average SVL and mid-body diameter for each species and the conspicuousness under the three threshold schemes. Node values and bars in the tree indicate mean age and 95% confidence intervals for the age estimates, respectively. Posterior probabilities are indicated by coloured circles at the node. More conspicuously coloured species are indicated by closed yellow circles and less conspicuous ones by open circles under the three schemes (L, liberal; I, intermediate, S, strict).

Morphometric data

We collected morphological measurements from specimens collected during our field sampling and from museum specimens deposited at the Bombay Natural History Society (BNHS) and ZSI-WGRC. The following 17 morphometric measurements were taken from each specimen: SVL, snout-to-vent length; TL, tail length; MD, mid-body diameter; MD/SVL, girth-to-length ratio; VW, width at vent; HL, head length; HW, head width; RL, rostral length; ED, eye diameter; OL, ocular length; IOL, interorbital length; SL, snout length; FL, frontal length; FW, frontal width; PL, parietal length; PW, parietal width; IPS, length of parietal suture (for definitions, see Supporting Information, Table S6). All measurements were taken using a digital vernier calliper (Yuri Silver, Japan) to the nearest 0.01 mm, except for the SVL, which was measured to the nearest 1 mm. We collected data from two to six specimens of each species, except for six species for which we could obtain data from only one specimen.

Phylogenetic comparative analysis

Phylogenetic signal in morphological traits

We carried out all our analyses in R v.3.5.2 (R Core Team, 2016). To test if phylogenetically related species have similar morphologies, we measured the phylogenetic signal in each of the morphological variables using Pagel's lambda (λ) (Pagel, 1997, 1999) and Blomberg's K (Blomberg *et al.*, 2003) employing the *phylosig* function in the 'phytools' v. 0.6–60 package (Revell, 2012). Pagel's λ ranges from 0 to 1 and indicates the degree of phylogenetic relatedness between species that possess a particular trait. Thus, if λ = 1, it indicates that the trait of interest has a strong phylogenetic signal and approximates a Brownian motion (BM) model of trait evolution. Similarly, K = 1 indicates a fit with a BM model, while large values (>> 1), indicate that traits of close relatives are more similar than expected under BM.

Correlation between conspicuousness and body size

To test the general relationship between colouration and body size in *Uropeltis* snakes, we checked if the overall conspicuousness score (ΣCS_i) was correlated with average SVL. We also checked if ΣCS_i was correlated with the average mid-body diameter (MD). To account for the statistical non-independence of our data due to phylogenetic relatedness, we estimated the phylogenetic independent contrasts (PIC) for ΣCS_i and the body size measures using the R package 'ape' v.5.2 (Paradis & Schliep, 2018). We then regressed the PICs for ΣCS_i with the PICs of SVL and mid-body diameter through the origin.

To further examine the relationship between colouration and morphology, we size-corrected the average body and head measurements by carrying out a phylogenetic regression on SVL using the *phyl.resid* functions in 'phytools'. We then carried out a phylogenetic principal component analysis (pPCA) using the *phyl.pca* function in 'phytools', after which we performed a phylogenetic generalized least square (PGLS) regression of the first three principal components (PCs). The PGLS was carried out to determine if morphological variables predicted the overall conspicuousness score of species. We fit three models where the PCs predict the conspicuousness and a null model where the conspicuousness is not predicted by morphology, using the *phylolm* function in the R package 'phylolm' v.2.6 (Ho *et al.*, 2018) and compared the models using Akaike Information Criterion (AIC).

Conspicuousness and rates of morphological evolution

To evaluate if the rates of morphological evolution are elevated for species with more conspicuous colouration, we compared the fit of different single and multi-rate models of trait evolution to our data. We used the package 'mvMORPH v.1.1.0 (Clavel *et al.*, 2015) to fit different multivariate evolutionary models using the three PCs obtained from a pPCA of the scaled size-corrected body and head measurements. To further test the influence of conspicuousness specifically on rates of head shape evolution, we performed pPCA on just the scaled size-corrected head measurements and fit different multivariate evolutionary models using the first three PCs. Head measurements were size-corrected using a phylogenetic regression on SVL using the *phyl.resid* functions in 'phytools'. We fit four alternate models: (1) a neutral Brownian motion (BM) model, wherein there is no association between colouration and head morphology; (2) a multi-rate Brownian motion model (BMM), where the rate of evolution varied between species with less and more conspicuous colouration; (3) an Ornstein–Uhlenbeck model (OU), where head morphology is not associated with colouration, but all species are pulled towards a single optimum; and (4) a multi-rate OU model (OUM), with two optima associated with species having less and more conspicuous colouration. For each model, we also compared the fit between an unconstrained model and three constrained models to test for the independent evolution or phenotypic integration of morphological traits. We used three parameter constraints: (1) 'equal model', where the three PCs covary and have equal variance; (2) 'diagonal model', where there is no evolutionary covariance between the three PCs but they have different variances; and (3) 'equal-diagonal', where there is no covariance between the three PCs and they have equal variance. We fit these multivariate evolutionary models using the *mvBM* and *mvOU* functions implemented in the package 'mvMORPH' v.1.1.0. We compared these models using AIC values corrected for small sample sizes (AICc) and selected the model that best fit our data. We carried out this analysis using the three conspicuousness threshold schemes (liberal, intermediate and strict) to test that all threshold schemes reflected the same evolutionary model. To further test if rates of head morphology are significantly different between less and more conspicuous species, we estimated the evolutionary rates for high-dimensional multivariate date (σ^2_{mult}) between the two groups and the rank-ordered ratio between the two rates. We then compared the observed ratio of evolutionary rate to a distribution of ratios obtained under a model where there is no difference in the rates of head-shape evolution between groups by simulating phenotypic data for 100 000 iterations. We performed this analysis using the *compare.evol.rates* function in the 'geomorph' package (Adams & Otárola-Castillo, 2013) for the three conspicuousness schemes.

RESULTS

Phylogenetic analysis and divergence dating

The topologies from the MrBayes and BEAST analyses were largely consistent with each other, with relationships between species being well resolved with high support (Fig. 1; Supporting Information, Fig. S2). The age estimates recovered for *Uropeltis* are similar to those in Cyriac & Kodandaramaiah (2017). The divergence date estimates indicate that the clade originated *c*. 20 million years before present, with deep divergences between most species (Fig. 1).

Phylogenetic signal in morphological traits

We find that there is weaker phylogenetic signal in *Uropeltis* morphology than predicted under a BM model for most variables, but phylogenetic signal is significantly high for few body and head shape variables (Supporting Information, Table S7). Both Pagel's λ and Blomberg's K indicate significantly strong phylogenetic signal for the girth-to-length ratio (λ = 0.87, $P < 0.0001$; K = 1.47, $P = 0.001$) and eye diameter (λ = 0.50, $P = 0.0279$; K = 0.60, $P = 0.033$) (Supporting Information, Table S7).

Correlation between conspicuousness and body size

The regression of the phylogenetic independent contrasts indicates a positive correlation between the

overall conspicuousness score and average mid-body diameter (R^2 = 0.1953, P = 0.03059), but there is no relationship between the overall conspicuous score and SVL (R^2 = 0.0999, P = 0.1323) (Fig. 2). Most of the variation in morphology is explained by the first three principal components (86.14% of variation). PC1 explains 53% of the variation and describes a thin and long body shape with short and narrow head morphology (Supporting Information, Table S8). PC2 explains *c*. 24% of the variation and mainly describes a reduced frontal width, which reflects a narrow head (Supporting Information, Table S6). PC3 explains only *c*. 9% of the variation and describes a short rostrum (supplementary Supporting Information, Table S8). To test if the conspicuousness score is associated with morphology, we used a PGLS analysis with the three PCs as predictor variables. The best-fit model, where all three PCs explain the conspicuousness of species, is better compared both to a model where only PC1 and PC2 explains overall conspicuousness (ΔAIC = 3.17) and to a null model where morphology did not predict colouration (ΔAIC = 5.3) (supplementary Supporting Information, Table S9). The best-fit model indicates that there is a significant decrease in the PC1 (estimate = –0.1805, t = –2.6796, P = 0.0144) and PC3 scores (estimate = –0.4500, t = –2.1928, P = 0.0403) with increased overall conspicuousness (Fig. 3). However, compared with the best-fit model, there is no strong evidence against a model where only PC1 explains conspicuousness (ΔAIC = 1.21). Nonetheless, both the best-fit model and the two alternate models indicate that PC1 significantly explains the overall conspicuousness score (Supporting Information, Table S9).

Conspicuousness and rates of morphological evolution

To test if the rates for morphological evolution differ between less and more conspicuous lineages in the three conspicuousness threshold schemes, we fit different single and multi-rate models of trait evolution. We find that an OU model with one optimum, best fit the data in the intermediate and strict schemes, while a multi-rate Brownian motion model best fit the data under the liberal threshold scheme (Supporting Information, Table S10). However, in the liberal scheme, the best-fit model is not significantly different from the OU model with one optimum (ΔAICc = 0.65) (Supporting Information, Table S10).

The phylogenetic PCA on the head morphology indicates that most of the variation in *Uropeltis* is explained by the first three PCs (90.25% of the variation). The first PC explains *c*. 49% of the variation and describes a short, narrow head (Supporting Information, Table S11). PC2 explains *c*. 31% of the variation and describes a larger frontal width, while PC3 explains *c*. 10% of the variation and describes a long

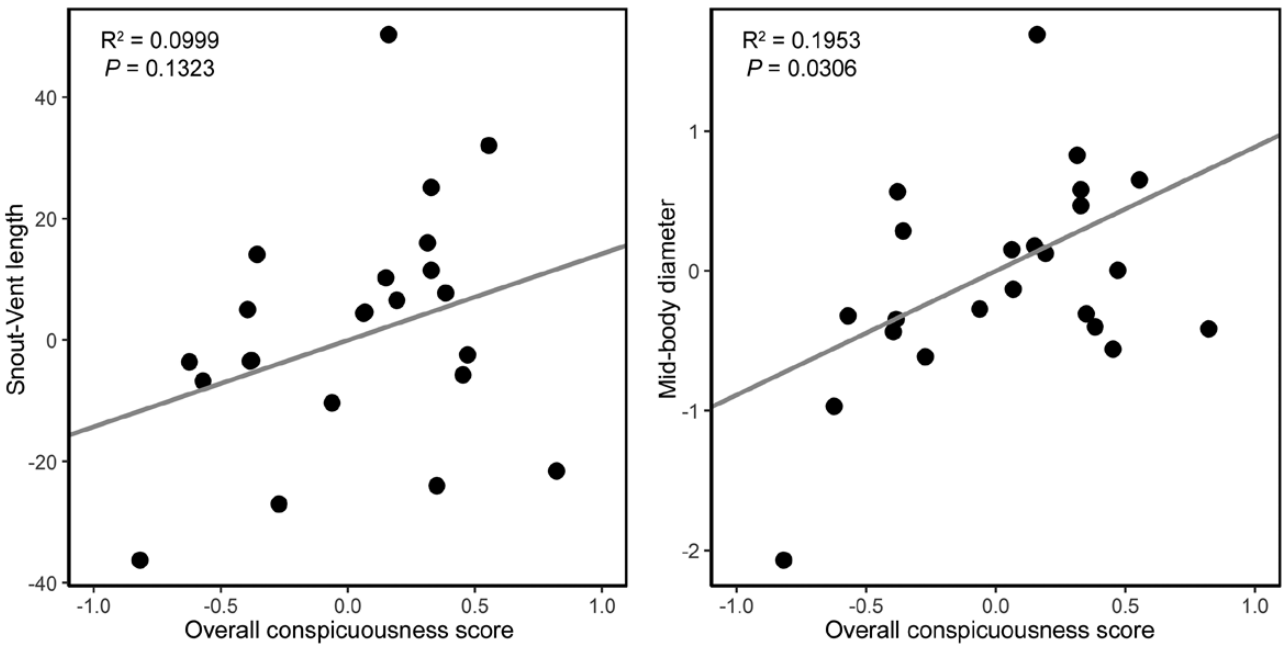

Figure 2. Relationship between the overall conspicuousness scores and average snout–vent length (SVL), and between the overall conspicuousness scores and mid-body diameter (MD), in *Uropeltis* species estimated by phylogenetic independent contrasts under a Brownian motion model of evolution.

snout and rostral scale (Supporting Information, Table S11). Fitting different single and multi-rate models of trait evolution on the three head-shape PCs, we find that the multi-rate Brownian motion (BMM) model fit our data significantly better under all three threshold schemes (ΔAICc > 4) (Supporting Information, Table S12). Further, the BMM unconstrained model better explains our data, as opposed to other constrained models (ΔAICc > 4). Parameter estimation of the best-fit BMM model indicates that, although there is not much difference in the rates of morphological evolution for PC1 in all three threshold schemes, the rates of morphological evolution for PC2 is considerably greater for species with more colouration under all three threshold schemes (Table 1). Rates of morphological evolution for PC3 are also higher for species having more conspicuous colouration, but only under the intermediate and strict threshold schemes (Table 1). The estimated evolutionary rates for the high-dimensional multivariate head-shape data (σ^2_{mult}) also indicate significantly different evolutionary rates for species with less and more colouration under the intermediate scheme ($\sigma^2_{mult.a}/\sigma^2_{mult.b}$ = 1.9366, P = 0.0290) (Table 2). The parameter estimates indicate that the rates of head-shape evolution under the intermediate scheme were about two times higher in species with more conspicuous colouration than species with less conspicuous colouration ($\sigma^2_{less\ conspicuous}$ = 0.0543, $\sigma^2_{more\ conspicuous}$ = 0.1052). Although the observed ratio of evolutionary rates between the two groups ($\sigma^2_{mult.a}/\sigma^2_{mult.b}$) is only marginally significantly different from the ratio generated under a null distribution for the liberal threshold scheme, the rates of head-shape evolution estimated under the liberal scheme was higher for species with more colouration ($\sigma^2_{mult.a}/\sigma^2_{mult.b}$ = 1.7807, P = 0.0598, $\sigma^2_{less\ conspicuous}$ = 0.0548, $\sigma^2_{more\ conspicuous}$ = 0.0976) (Table 2).

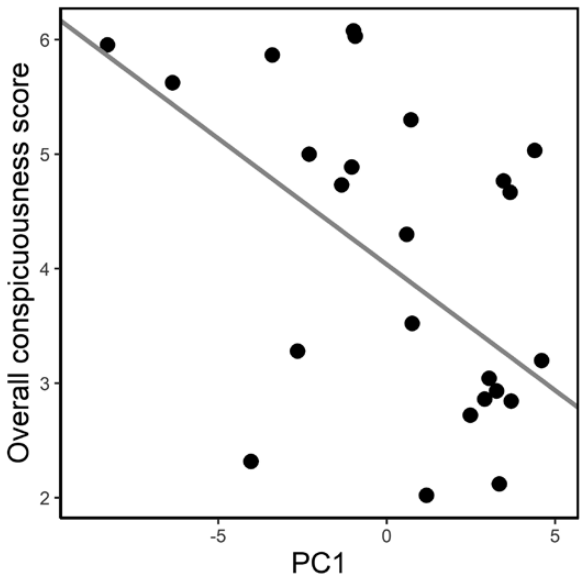

Figure 3. Correlation between the overall conspicuousness score and first principal component (PC1) from the pPCA analysis of the head and body size measurements.

DISCUSSION

Phylogenetic signal and morphology

Among the 17 traits measured, girth-to-length ratio (MD/SVL) has the highest phylogenetic signal and is one of the few traits with significant phylogenetic signal (λ = 0.87, P = 7.46e-06; Blomberg's K > 1, P = 0.001) (Supporting Information, Table S7). Strong phylogenetic signal, where closely related species have more similar traits than expected under Brownian motion, is indicative of strong niche conservatism due to stabilizing selection or environmental and developmental constraints (Wiens & Graham, 2005; Cooper *et al.*, 2010; Wiens *et al.*, 2010). Studies have suggested that the work required for a fossorial species to burrow into the soil increases exponentially with its cross-sectional area (Gans, 1960; Navas *et al.*, 2004; Wu *et al.*, 2015) and hence the girth-to-length ratio can determine the burrowing ability of a fossorial species (Navas *et al.*, 2004). Thus, it is expected that traits that overcome the energetic constraints

Table 1. Rates of morphological evolution (σ^2_{mult}) estimated for the best-fit model explaining head-shape evolution in *Uropeltis* under the three threshold schemes of conspicuousness. The best-fit model in all cases is the unconstrained multi-rate Brownian motion (BMM) model for all three principal components (PCs) explaining variation in head shape

Threshold scheme	Best-fit model	Trait	PC1	PC2	PC3
Liberal scheme	BMM unconstrained	Less conspicuous	0.4795	0.0283	0.0875
		More conspicuous	0.4452	0.4588	0.0828
Intermediate scheme	BMM unconstrained	Less conspicuous	0.4155	0.0225	0.0852
		More conspicuous	0.5330	0.6896	0.1093
Strict scheme	BMM unconstrained	Less conspicuous	0.4493	0.0353	0.0846
		More conspicuous	0.3905	0.7844	0.1297

Table 2. Parameter estimates for the rate ordered observed rate ratio and the evolutionary rates for high-dimensional multivariate head shape data (σ^2_{mult}) between the more and less conspicuous species under the three threshold conspicuousness schemes (liberal, intermediate and strict). The *P* values were obtained by comparing the observed rate ratio with a null distribution obtained by simulating phenotypic data for 100 000 iterations and bold values are < 0.05

Parameter	Liberal	Intermediate	Strict
Observed rate ratio	1.7803	1.9366	1.0556
P value	0.0598	**0.0290**	0.8843
$\sigma^2_{less\ conspicuous}$	0.0548	0.0543	0.0806
$\sigma^2_{more\ conspicuous}$	0.0976	0.1052	0.0764

associated with burrowing, such as girth-to-length ratio, will experience strong stabilizing selection and have reduced lability as indicated by the strong phylogenetic signal.

Conspicuousness and body size

Evolution of conspicuous warning colourations are frequently thought to be associated with increased body size, either because larger size increases the efficacy of learning warning signals (Gamberale & Tullberg, 1996; Forsman & Merilaita, 1999) or because larger prey are more nutritious and easily visible and, therefore, experience greater selection pressure to evolve alternate defences (Penney *et al.*, 2012; Hossie *et al.*, 2015). Interestingly, in the regression of the phylogenetic independent contrasts, we find no significant correlation between overall colouration and snout–vent length. Although many studies support a positive conspicuousness–body size relationship (Forsman & Merilaita, 1999; Hagman & Forsman, 2003; Rudh, 2013; Kang *et al.*, 2017; Winebarger *et al.*, 2018; Loeffler-Henry *et al.*, 2019), there are several studies that show a negative association between conspicuousness and body size (Nilsson & Forsman, 2003; Cheney *et al.*, 2014; Winebarger *et al.*, 2018), possibly because of the confounding influence of other selection pressures on body size. However, as expected, we found a strong positive correlation between colouration and absolute girth. The PGLS analysis also indicates that the overall colouration is significantly associated with morphotypes that influence burrowing ability, i.e. less conspicuously coloured species are thinner and longer and have narrower heads, while species with more conspicuous colourations are larger bodied and with wider heads (Fig. 3).

In concert with our hypothesis that warning signals in uropeltid snakes allow greater surface activity, we find a strong association between the degree of warning colourations and more robust body forms. Although we have not specifically tested if large-bodied species are more surface-active, several studies indicate that fossorial species tend to be more elongate, with short, narrow heads in order to overcome the energetic costs of a burrowing lifestyle (Navas *et al.*, 2004; Shine & Wall, 2008; Camacho *et al.*, 2015; Wu *et al.*, 2015). Experiments have shown that skull size strongly influences digging performance in head-first burrowing species. Species with larger and wider heads tend to have lower burrowing speeds (Teodecki *et al.*, 1998; Navas *et al.*, 2004; Vanhooydonck *et al.*, 2010; Hohl *et al.*, 2017). Since the net cost of burrowing into the soil decreases with burrowing rates (Wu *et al.*, 2015), it is intuitive that species with specializations that improve burrowing performance, such as an elongate body and small, narrow heads, are able to dig deeper into the soil than more robust species. Although there are few studies that have recorded the depth at which these burrowing morphotypes occur, observations have suggested that elongate species with narrower heads have better burrowing performance and can dig deeper into the soil (Navas *et al.*, 2004; Camacho *et al.*, 2015; Hohl *et al.*, 2017). For instance, in the fossorial amphisbaenian lizards, it was found that the more elongate and more specialized species were found at greater soil depths than shorter, more robust species (Gomes *et al.*, 2009). Further, greater axial muscle mass increases locomotor performance on the surface. Studies have shown that crawling speed on the surface and swimming speed in snakes increase with body weight up to a certain length (Heckrotte, 1967; Kelley *et al.*, 1997; Webb *et al.*, 2001). Given that large-bodied snakes have advantages with regard to movement on the surface, it is not surprising that larger bodied *Uropeltis* species tend to possess a greater extent of warning colourations. Similar trends have been observed in fossorial caecilians, where the presence of conspicuous colouration was associated with ecological characters indicative of above-ground movement (Wollenberg & Measey, 2009).

Conspicuousness and rates of morphological evolution

Fitting models of trait evolution, using the three principal components obtained by analysing all morphological variables, indicates that an OU model with one optimum is the best-fit model. Interestingly, including only the head-shape principal components indicates that a multi-rate Brownian motion model best explains our data under all colour-threshold schemes. Such multiregime models of trait evolution are usually expected when a trait opens new niche space that can be filled up by new species (Yoder *et al.*, 2010). Under

such cases, it is expected that the rates of trait evolution are accelerated in lineages that acquire the trait (O'Meara *et al.*, 2006; Yoder *et al.*, 2010). Accordingly, evolutionary rates are higher in species with more conspicuous colouration for PC2 (explained by the frontal width of the head) under all three schemes, while being higher only in the intermediate scheme for PC1 (describing overall head shape) and in the intermediate and strict schemes for PC3 (explained by the rostral and snout length) (Table 1). We also recover similar patterns when estimating the evolutionary rates for the high-dimensional multivariate head-shape data, where the rates of head-shape evolution are higher in more conspicuously coloured lineages than in less conspicuously coloured ones. Overall, we find that the evolution of conspicuous colourations in *Uropeltis* species is linked with larger body girth and wider heads, and is also associated with accelerated rates of head shape evolution associated with more surface activity and reduced constraints associated with fossoriality. We acknowledge that the analysis performed is limited in that we have not tested whether warning colouration evolved before morphological change, and thus we cannot draw a causal relationship for the correlation between conspicuousness and morphological evolution. However, it should be noted that most *Uropeltis* species (and almost all species included in the analyses) have some amount of warning colourations on the ventral (see Supporting Information, Fig. S3), dorsal or lateral sides, which suggests that the evolution of warning colouration preceded morphological changes in *Uropeltis*.

Our results suggest that the variation observed in the rates of head-shape evolution are highly dependent on the coding of conspicuousness. The rate estimates from the high-dimensional multivariate head-shape data indicate significant differences in the rates between less and more conspicuous lineages, only for the intermediate coding scheme, while the difference was only marginally significant for the liberal scheme. However, it should be noted that the rates of head-shape evolution are considerably higher in more conspicuous lineages for PC2 (described by frontal width) and for PC3 (describing snout and rostral length) under most coding schemes (Table 1). Fossorial reptiles show considerable variation in the shape and arrangement of rostral elements and the nasofrontal region of the cranium, both of which could have functional significance (Cundall, 1995; Olori & Bell, 2012). In head-first burrowing reptiles, the shape and angulation of the rostral are associated with the resistance experienced in the microhabitat (Barros *et al.*, 2011). On the other hand, the frontals in the cranium of basal fossorial snakes are articulated with the rest of the snout in such a way that it allows the independent movement of the entire snout at the nasofrontal joint (Cundall & Rossman, 1993; Cundall, 1995; Rieppel, 2007). Such an arrangement enables these snakes to consume larger prey with small diameters (Greene, 1983; Cundall, 1995). Thus, the high rates of morphological evolution among more conspicuous lineages of *Uropeltis* recovered for the frontal width, and the rostral and snout lengths, could potentially reflect changes associated with burrowing and shifts towards larger elongated prey.

Predation pressure is a strong selective force that can lead to divergent selection and ecological speciation (McPeek, 1997; Nosil, 2004; Rundle & Nosil, 2005; Vamosi, 2005; Langerhans *et al.*, 2007; Meyer & Kassen, 2007). Predation pressure can also influence rates of phenotypic evolution, especially in traits that are involved in defensive function (Broeckhoven *et al.*, 2016). On the other hand, the elimination of predators from an environment can promote lineage diversification through divergence of traits that were previously constrained by predator-induced selection (Schluter, 1988; Meyer & Kassen, 2007; Heinen-Kay & Langerhans, 2013; Runemark *et al.*, 2014). For instance, Runemark *et al.* (2014) showed that lizards present on islets with reduced predation pressure were large and less cryptic than their mainland counterparts that experienced higher predation. Similarly, theory suggests that antipredatory defences that provide prey with a predator-free space can open up adaptive zones, thereby facilitating niche expansion and, in turn, lineage diversification (Merilaita & Tullberg, 2005; Speed *et al.*, 2010). A few studies that have tested this escape-and-radiate hypothesis have indicated that the evolution of defensive traits have increased lineage diversification (Ehrlich & Raven, 1964; Farrell *et al.*, 1991; Przeczek *et al.*, 2008; Agrawal *et al.*, 2009; Santos *et al.*, 2014; Weber & Agrawal, 2014; Arbuckle & Speed, 2015). It has been suggested that the evolution of defences allows access to other resources that would normally be inaccessible to prey in the presence of high predator pressure and thus increase niche space (Wallace, 1889; Stamp & Wilkens, 1993; Merilaita & Tullberg, 2005; Speed *et al.*, 2010), eventually leading to further diversification (Ehrlich & Raven, 1964; Agrawal *et al.*, 2009; Weber & Agrawal, 2014; Arbuckle & Speed, 2015). A few studies have supported this idea and shown that species with warning colourations tend to be associated with traits that indicate broader niche breadth (Bowers, 1993; Pröhl & Ostrowski, 2011; Rudh *et al.*, 2012; Arbuckle *et al.*, 2013). For example, it has been shown that populations of poison dart frogs that are more conspicuous tend to be more aggressive and exploratory and spend less time being hidden and more time foraging (Pröhl & Ostrowski, 2011; Rudh *et al.*, 2012). It was also shown that conspicuously coloured frogs had greater acoustic diversity and higher speciation rates than more cryptic species (Santos *et al.*, 2014). Our finding that

the evolution of warning colourations in *Uropeltis* is associated with morphological niche divergence adds to our understanding of how the evolution of defences can increase niche space by showing that the evolution of conspicuous colourations is linked with larger body size and is also associated with accelerated rates of head-shape evolution. We also highlight how such defensive strategies can alter the interaction of species with its environment and introduce them to other selective pressures, in our case by reducing the morphological constraints imposed by fossoriality and thereby promoting morphological diversification.

AUTHOR CONTRIBUTIONS

VPC conceived the study, designed the experiment, carried out the molecular work, collected morphological data, analysed the data and drafted the manuscript. UK provided materials and critically revised the manuscript.

DATA ACCESSIBILITY

DNA sequences: see electronic Supporting Information, Table S2. Phylogenetic and morphometric data: https://figshare.com/s/8601fa5a1e8a60c507d2

ACKNOWLEDGEMENTS

We thank the Kerala Forest and Wildlife Department for providing permits to VPC (order no. WL10-7451/2013). We thank all the participants who took part in scoring the colouration of uropeltid snakes. We thank David Gower for discussions on uropeltid colourations. We also thank David Gower and Filipa Shampaio for their help with lab work and sequencing. We also thank Dr P. M. Sureshan, Dr Muhamed Jafer Palot, Rahul Khot and Sameer Bajaru for providing access to museum specimens at ZSI-WGRC and BNHS. We thank Omkar Andheri, Nikhil Modak and Dipika Valsarajan for their help during examining museum specimens at BNHS. We thank Umesh P. K., Arjun C. P., Jins V. J. and Shubhankar Deshpande for providing images of *Uropeltis* species.

COMPETING INTEREST

The authors declare that they have no conflict of interest.

FUNDING

This study was funded by intramural grants from IISER Thiruvananthapuram and an INSPIRE Faculty Award from the Department of Science and Technology (DST/INSPIRE/04/2013/000476) to UK.

REFERENCES

Adams DC, **Otárola-Castillo E. 2013.** Geomorph: an R package for the collection and analysis of geometric morphometric shape data. *Methods in Ecology and Evolution* **4:** 393–399.

Agrawal AA, **Fishbein M**, **Halitschke R**, **Hastings AP**, **Rabosky DL**, **Rasmann S. 2009.** Evidence for adaptive radiation from a phylogenetic study of plant defenses. *Proceedings of the National Academy of Sciences of the USA* **106:** 18067–18072.

Arbuckle K, **Speed MP. 2015.** Antipredator defenses predict diversification rates. *Proceedings of the National Academy of Sciences of the USA* **112:** 13597–13602.

Arbuckle K, **Brockhurst M**, **Speed MP. 2013.** Does chemical defence increase niche space? A phylogenetic comparative analysis of the Musteloidea. *Evolutionary Ecology* **27:** 863–881.

Aronsson M, **Gamberale-Stille G. 2012.** Evidence of signaling benefits to contrasting internal color boundaries in warning colouration. *Behavioral Ecology* **24:** 349–354.

Barros FC, **Herrel A**, **Kohlsdorf T. 2011.** Head shape evolution in Gymnophthalmidae: does habitat use constrain the evolution of cranial design in fossorial lizards? *Journal of Evolutionary Biology* **24:** 2423–2433.

Blomberg SP, **Garland T**, **Ives AR. 2003.** Testing for phylogenetic signal in comparative data: behavioral traits are more labile. *Evolution* **57:** 717–745.

Bond AB, **Kamil AC. 2006.** Spatial heterogeneity, predator cognition, and the evolution of color polymorphism in virtual prey. *Proceedings of the National Academy of Sciences of the USA* **103:** 3214–3219.

Bouckaert R, **Heled J**, **Kühnert D**, **Vaughan T**, **Wu CH**, **Xie D**, **Suchard MA**, **Rambaut A**, **Drummond AJ. 2014.** BEAST 2: a software platform for Bayesian evolutionary analysis. *PLoS Computational Biology* **10:** e1003537.

Bowers MD. 1993. Aposematic caterpillars: life-styles of the warningly colored and unpalatable. In: Stamp NE, Casey TM, eds. *Caterpillars: ecological and evolutionary constraints on foraging*. New York: Chapman & Hall, 331–371.

Broeckhoven C, **Diedericks G**, **Hui C**, **Makhubo BG**, **Mouton P le FN. 2016.** Enemy at the gates: rapid defensive trait diversification in an adaptive radiation of lizards. *Evolution* **70:** 2647–2656.

Camacho A, **Pavão R**, **Moreira CN**, **Pinto ACB**, **Navas CA**, **Rodrigues MT. 2015.** Interaction of morphology, thermal physiology and burrowing performance during the evolution of fossoriality in Gymnophthalmini lizards. *Functional Ecology* **29:** 515–521.

Cheney KL, **Cortesi F**, **How MJ**, **Wilson NG**, **Blomberg SP**, **Winters AE**, **Umanzör S**, **Marshall NJ. 2014.** Conspicuous visual signals do not coevolve with increased body size in marine sea slugs. *Journal of Evolutionary Biology* **27:** 676–687.

Clavel J, **Escarguel G**, **Merceron G. 2015.** MvMORPH: an R package for fitting multivariate evolutionary models to morphometric data. *Methods in Ecology and Evolution* **6:** 1311–1319.

Cooper N, **Jetz W**, **Freckleton RP. 2010.** Phylogenetic comparative approaches for studying niche conservatism. *Journal of Evolutionary Biology* **23:** 2529–2539.

Cummins CA, **McInerney JO. 2011.** A method for inferring the rate of evolution of homologous characters that can potentially improve phylogenetic inference, resolve deep divergence and correct systematic biases. *Systematic Biology* **60:** 833–844.

Cundall D. 1995. Feeding behaviour in *Cylindrophis* and its bearing on the evolution of alethinophidian snakes. *Journal of Zoology* **237:** 353–376.

Cundall D, **Rossman DA. 1993.** Cephalic anatomy of the rare Indonesian snake *Anomochilus weberi*. *Zoological Journal of the Linnean Society* **109:** 235–273.

Cyriac VP, **Kodandaramaiah U. 2017.** Paleoclimate determines diversification patterns in the fossorial snake family Uropeltidae Cuvier, 1829. *Molecular Phylogenetics and Evolution* **116:** 97–107.

Cyriac VP, **Kodandaramaiah U. 2018.** Digging their own macroevolutionary grave: fossoriality as an evolutionary dead end in snakes. *Journal of Evolutionary Biology* **31:** 587–598.

Cyriac VP, **Kodandaramaiah U. 2019a.** Conspicuous colours reduce predation rates in fossorial uropeltid snakes. *PeerJ* **7:** e7508.

Cyriac VP, **Kodandaramaiah U. 2019b.** Don't waste your time: predators avoid prey with conspicuous colours that signal long handling time. *Evolutionary Ecology* **33:** 625–636.

Edgar RC. 2004. MUSCLE: multiple sequence alignment with high accuracy and high throughput. *Nucleic Acids Research* **32:** 1792–1797.

Ehrlich PR, **Raven PH. 1964.** Butterflies and plants: a study in coevolution. *Evolution* **18:** 586–608.

Farrell BD, **Dussourd DE**, **Mitter C. 1991.** Escalation of plant defense: do latex and resin canals spur plant diversification? *The American Naturalist* **138:** 881–900.

Forsman A, **Merilaita S. 1999.** Fearful symmetry: pattern size and asymmetry affects aposematic signal efficacy. *Evolutionary Ecology* **13:** 131–140.

Gamberale G, **Tullberg BS. 1996.** Evidence for a more effective signal in aggregated aposematic prey. *Animal Behaviour* **52:** 597–601.

Gamer M, Lemon J, Fellows I, Singh P. 2019. irr: Various Coefficients of Interrater Reliability and Agreement. R package version 0.84.1. Available at: https://CRAN.R-project.org/package=irr (accessed 24 February 2020).

Gans C. 1960. Studies on amphisbaenids (Amphisbaenia, Reptilia). 1, A taxonomic revision of the Trogonophinae, and a functional interpretation of the amphisbaenid adaptive pattern. *Bulletin of the American Museum of Natural History* **119:** 133–204.

Gans C. 1968. Relative success of divergent pathways in amphisbaenian specialization. *The American Naturalist* **102:** 345–362.

Gans WS, **Dessauer HC**, **Baic D. 1978.** Axial differences in the musculature of uropeltid snakes: the freight-train approach to burrowing. *Science* **199:** 189–192.

Gomes JO, **Maciel AO**, **Costa JC**, **Andrade GV. 2009.** Diet composition in two sympatric amphisbaenian species *(Amphisbaena ibijara* and *Leposternon polystegum*) from the Brazilian Cerrado. *Journal of Herpetology* **43:** 377–384.

Greene HW. 1979. Behavioral convergence in the defensive displays of snakes. *Experientia* **35:** 747–748.

Greene HW. 1983. Dietary correlates of the origin and radiation of snakes. *American Zoologist* **23:** 431–441.

Greene HW. 1988. Antipredator mechanisms in reptiles. *Biology of the Reptilia* **16:** 1–152.

Gurevitch J, **Morrison JA**, **Hedges LV. 2000.** The interaction between competition and predation: a meta-analysis of field experiments. *The American Naturalist* **155:** 435–453.

Hagman M, **Forsman A. 2003.** Correlated evolution of conspicuous colouration and body size in poison frogs (Dendrobatidae). *Evolution* **57:** 2904–2910.

Heckrotte C. 1967. Relations of body temperature, size, and crawling speed of the common garter snake, *Thamnophis s. sirtalis*. *Copeia* **1967.** 759–763.

Heinen-Kay JL, **Langerhans RB. 2013.** Predation-associated divergence of male genital morphology in a livebearing fish. *Journal of Evolutionary Biology* **26:** 2135–2146.

Ho LST, **Ane C**, **Lachlan R**, **Tarpinian K**, **Feldman R**, **Yu Q**, **Van der Bijl W. 2018.** *Package 'phylolm', v.2.6*. Available at: http://mirror.psu.ac.th/pub/cran/web/packages/phylolm/phylolm.pdf (accessed 09 April 2019).

Hohl L dos SL, **de Castro Loguercio MF**, **Sicuro FL**, **de Barros-Filho JD**, **Rocha-Barbosa O. 2017.** Body and skull morphometric variations between two shovel-headed species of Amphisbaenia (Reptilia: Squamata) with morphofunctional inferences on burrowing. *PeerJ* **5:** e3581.

Hossie TJ, **Skelhorn J**, **Breinholt JW**, **Kawahara AY**, **Sherratt TN. 2015.** Body size affects the evolution of eyespots in caterpillars. *Proceedings of the National Academy of Sciences of the USA* **112:** 6664–6669.

Houston AI, **Stevens M**, **Cuthill IC. 2007.** Animal camouflage: compromise or specialize in a 2 patch-type environment? *Behavioral Ecology* **18:** 769–775.

Kang C, **Zahiri R**, **Sherratt TN. 2017.** Body size affects the evolution of hidden colour signals in moths. *Proceedings of the Royal Society B: Biological Sciences* **284:** 20171287.

Kelley KC, **Arnold SJ**, **Gladstone J. 1997.** The effects of substrate and vertebral number on locomotion in the garter snake *Thamnophis elegans*. *Functional Ecology* **11:** 189–198.

Khandekar A, **Gaitonde N**, **Roy P**, **Kunte K. 2019.** *Reptiles of India, v.1.22*. Indian Foundation for Butterflies. Available at: https://www.indianreptiles.org (accessed 06 March 2019).

Kumar S, **Stecher G**, **Tamura K. 2016.** MEGA7: molecular evolutionary genetics analysis version 7.0 for bigger datasets. *Molecular Biology and Evolution* **33:** 1870–1874.

Lanfear R, **Frandsen PB**, **Wright AM**, **Senfeld T**, **Calcott B. 2016.** PartitionFinder 2: new methods for selecting partitioned models of evolution for molecular and

morphological phylogenetic analyses. *Molecular Biology and Evolution* **34:** 772–773.

Langerhans RB, **Gifford ME**, **Joseph EO. 2007.** Ecological speciation in Gambusia fishes. *Evolution* **61:** 2056–2074.

Loeffler-Henry K, **Kang C**, **Sherratt TN. 2019.** Consistent associations between body size and hidden contrasting color signals across a range of insect taxa. *The American Naturalist* **194:** 28–37.

Mappes J, **Marples N**, **Endler JA. 2005.** The complex business of survival by aposematism. *Trends in Ecology & Evolution* **20:** 598–603.

McPeek MA. 1997. Measuring phenotypic selection on an adaptation: lamellae of damselflies experiencing dragonfly predation. *Evolution* **51:** 459–466.

Merilaita S, **Lind J. 2005.** Background-matching and disruptive colouration, and the evolution of cryptic colouration. *Proceedings of the Royal Society B: Biological Sciences* **272:** 665–670.

Merilaita S, **Tullberg BS. 2005.** Constrained camouflage facilitates the evolution of conspicuous warning colouration. *Evolution* **59:** 38–45.

Merilaita S, **Tuomi J**, **Jormalainen V. 1999.** Optimization of cryptic colouration in heterogeneous habitats. *Biological Journal of the Linnean Society* **67:** 151–161.

Merilaita S, **Lyytinen A**, **Mappes J. 2001.** Selection for cryptic colouration in a visually heterogeneous habitat. *Proceedings of the Royal Society of London B: Biological Sciences* **268:** 1925–1929.

Meyer JR, **Kassen R. 2007.** The effects of competition and predation on diversification in a model adaptive radiation. *Nature* **446:** 432–435.

Miller MA, **Pfeiffer W**, **Schwartz T. 2010.** Creating the CIPRES Science Gateway for inference of large phylogenetic trees. In: *Proceedings of the Gateway Computing Environments Workshop (GCE)*. New Orleans: IEEE, 1–8.

Navas CA, **Antoniazzi MM**, **Carvalho JE**, **Chaui-Berlink JG**, **James RS**, **Jared C**, **Kohlsdorf T**, **Dal Pai-Silva M**, **Wilson RS. 2004.** Morphological and physiological specialization for digging in amphisbaenians, an ancient lineage of fossorial vertebrates. *Journal of Experimental Biology* **207:** 2433–2441.

Nevo E. 1979. Adaptive convergence and divergence of subterranean mammals. *Annual Review of Ecology and Systematics* **10:** 269–308.

Nilsson M, **Forsman A. 2003.** Evolution of conspicuous colouration, body size and gregariousness: a comparative analysis of lepidopteran larvae. *Evolutionary Ecology* **17:** 51–66.

Nosil P. 2004. Reproductive isolation caused by visual predation on migrants between divergent environments. *Proceedings of the Royal Society of London B: Biological Sciences* **271:** 1521–1528.

Olori JC, **Bell CJ. 2012.** Comparative skull morphology of uropeltid snakes (Alethinophidia: Uropeltidae) with special reference to disarticulated elements and variation. *PLoS One* **7:** e32450.

O'Meara BC, **Ané C**, **Sanderson MJ**, **Wainwright PC. 2006.** Testing for different rates of continuous trait evolution using likelihood. *Evolution* **60:** 922–933.

Pagel M. 1997. Inferring evolutionary processes from phylogenies. *Zoologica Scripta* **26:** 331–348.

Pagel M. 1999. Inferring the historical patterns of biological evolution. *Nature* **401:** 877.

Paradis E, **Schliep K. 2018.** Ape 5.0: an environment for modern phylogenetics and evolutionary analyses in R. *Bioinformatics* **35:** 526–528.

Penney HD, **Hassall C**, **Skevington JH**, **Abbott KR**, **Sherratt TN. 2012.** A comparative analysis of the evolution of imperfect mimicry. *Nature* **483:** 461.

Pipan T, **Lopez H**, **Oromi P**, **Polak S**, **Culver DC. 2010.** Temperature variation and the presence of troglobionts in terrestrial shallow subterranean habitats. *Journal of Natural History* **45:** 253–273.

Pröhl H, **Ostrowski T. 2011.** Behavioural elements reflect phenotypic colour divergence in a poison frog. *Evolutionary Ecology* **25:** 993–1015.

Przeczek K, **Mueller C**, **Vamosi SM. 2008.** The evolution of aposematism is accompanied by increased diversification. *Integrative Zoology* **3:** 149–156.

R Core Team. **2016.** *R: a language and environment for statistical computing*. Vienna: R Foundation for Statistical Computing.

Rambaut A, **Suchard MA**, **Xie D**, **Drummond AJ. 2014.** *Tracer, v.1.6*. Available at: http://beast.community/tracer (accessed 13 March 2019).

Revell LJ. 2012. Phytools: an R package for phylogenetic comparative biology (and other things). *Methods in Ecology and Evolution* **3:** 217–223.

Rieppel O. 1977. Studies on the skull of the Henophidia (Reptilia: Serpentes). *Journal of Zoology* **181:** 145–173.

Rieppel O. 2007. The naso-frontal joint in snakes as revealed by high-resolution X-ray computed tomography of intact and complete skulls. *Zoologischer Anzeiger, a Journal of Comparative Zoology* **246:** 177–191.

Rieppel OA, **Zaher H. 2002.** The skull of the Uropeltinae (Reptilia, Serpentes), with special reference to the otico-occipital region. *Bulletin of the Natural History Museum, Zoology* **68:** 123–130.

Ronquist F, **Teslenko M**, **Van der Mark P**, **Ayres DL**, **Darling A**, **Höhna S**, **Larget B**, **Liu L**, **Suchard MA**, **Huelsenbeck JP. 2012.** MrBayes 3.2: efficient Bayesian phylogenetic inference and model choice across a large model space. *Systematic Biology* **61:** 539–542.

Roscito JG, **Rodrigues MT. 2010.** Comparative cranial osteology of fossorial lizards from the tribe Gymnophthalmini (Squamata, Gymnophthalmidae). *Journal of Morphology* **271:** 1352–1365.

Rudh A. 2013. Loss of conspicuous colouration has co-evolved with decreased body size in populations of poison dart frogs. *Evolutionary Ecology* **27:** 755–767.

Rudh A, **Breed MF**, **Qvarnström A. 2012.** Does aggression and explorative behaviour decrease with lost warning colouration? *Biological Journal of the Linnean Society* **108:** 116–126.

Rundle HD, **Nosil P. 2005.** Ecological speciation. *Ecology Letters* **8:** 336–352.

Runemark A, **Brydegaard M**, **Svensson EI. 2014.** Does relaxed predation drive phenotypic divergence among insular populations? *Journal of Evolutionary Biology* **27:** 1676–1690.

Ruxton GD, **Sherratt TN**, **Speed MP. 2004.** *Avoiding attack: the evolutionary ecology of crypsis, warning signals and mimicry.* Oxford: Oxford University Press.

Santos JC, **Baquero M**, **Barrio-Amorós C**, **Coloma LA**, **Erdtmann LK**, **Lima AP**, **Cannatella DC. 2014.** Aposematism increases acoustic diversification and speciation in poison frogs. *Proceedings of the Royal Society B: Biological Sciences* **281:** 20141761.

Schluter D. 1988. Character displacement and the adaptive divergence of finches on islands and continents. *The American Naturalist* **131:** 799–824.

Shine R, **Wall M. 2008.** Interactions between locomotion, feeding, and bodily elongation during the evolution of snakes. *Biological Journal of the Linnean Society* **95:** 293–304.

Speed MP, **Brockhurst MA**, **Ruxton GD. 2010.** The dual benefits of aposematism: predator avoidance and enhanced resource collection. *Evolution: International Journal of Organic Evolution* **64:** 1622–1633.

Stamp NE, **Wilkens RT. 1993.** On the cryptic side of life: being unapparent to enemies and the consequences for foraging and growth of caterpillars. In: Stamp NE, Casey TM, eds. *Caterpillars: ecological and evolutionary constraints on foraging*. New York: Chapman & Hall, 283–330.

Stevens M, **Ruxton GD. 2012.** Linking the evolution and form of warning colouration in nature. *Proceedings of the Royal Society B: Biological Sciences* **279:** 417–426.

Teodecki EE, **Brodie Jr ED**, **Formanowicz Jr DR**, **Nussbaum RA. 1998.** Head dimorphism and burrowing speed in the African caecilian *Schistometopum thomense* (Amphibia: Gymnophiona). *Herpetologica* **54:** 154–160.

Vaidya G, **Lohman DJ**, **Meier R. 2011.** SequenceMatrix: concatenation software for the fast assembly of multi-gene datasets with character set and codon information. *Cladistics* **27:** 171–180.

Vamosi SM. 2005. On the role of enemies in divergence and diversification of prey: a review and synthesis. *Canadian Journal of Zoology* **83:** 894–910.

Vanhooydonck B, **Boistel R**, **Fernandez V**, **Herrel A. 2010.** Push and bite: trade-offs between burrowing and biting in a burrowing skink (*Acontias percivali*). *Biological Journal of the Linnean Society* **102:** 91–99.

Vorobyev M, **Marshall J**, **Osorio D**, **Hempel de Ibarra N**, **Menzel R. 2001.** Colourful objects through animal eyes. *Color Research & Application* **26:** S214–S217.

Wallace AR. 1889. *Darwinism: an exposition of the theory of natural selection with some of its applications.* London & New York: Macmillan & Co.

Webb JK, **Brown GP**, **Shine R. 2001.** Body size, locomotor speed and antipredator behaviour in a tropical snake (*Tropidonophis mairii*, Colubridae): the influence of incubation environments and genetic factors. *Functional Ecology* **15:** 561–568.

Weber MG, **Agrawal AA. 2014.** Defense mutualisms enhance plant diversification. *Proceedings of the National Academy of Sciences of the USA* **111:** 16442–16447.

Wiens JJ, **Graham CH. 2005.** Niche conservatism: integrating evolution, ecology, and conservation biology. *Annual Review of Ecology, Evolution, and Systematics* **36:** 519–539.

Wiens JJ, **Ackerly DD**, **Allen AP**, **Anacker BL**, **Buckley LB**, **Cornell HV**, **Damschen EI**, **Davies TJ**, **Grytnes JA**, **Harrison SP**, **Hawkins BA**, **Holt RD**, **McCain CM**, **Stephens PR. 2010.** Niche conservatism as an emerging principle in ecology and conservation biology. *Ecology Letters* **13:** 1310–1324.

Winebarger MM, **Siefferman LM**, **Gangloff MM**, **Osbourn MS**, **Pugh MW. 2018.** Body size is positively correlated with conspicuous colouration in *Ambystoma salamanders*, negatively correlated with conspicuous colouration in *Plethodon* salamanders. *Frontiers in Ecology and Evolution* **6:** 143.

Wollenberg KC, **Measey CJ. 2009.** Why colour in subterranean vertebrates? Exploring the evolution of colour patterns in caecilian amphibians. *Journal of Evolutionary Biology* **22:** 1046–1056.

Wu NC, **Alton LA**, **Clemente CJ**, **Kearney MR**, **White CR. 2015.** Morphology and burrowing energetics of semi-fossorial skinks (*Liopholis* spp.). *Journal of Experimental Biology* **218:** 2416–2426.

Yoder JB, **Clancey E**, **Des Roches S**, **Eastman JM**, **Gentry L**, **Godsoe W**, **Hagey TJ**, **Jochimsen D**, **Oswald BP**, **Robertson J. 2010.** Ecological opportunity and the origin of adaptive radiations. *Journal of Evolutionary Biology* **23:** 1581–1596.

SUPPORTING INFORMATION

Additional Supporting Information may be found in the online version of this article at the publisher's web-site.

Table S1. Primers used for amplification of genes in *Uropeltis* (sequences are from 5'–3' direction). Both forward and reverse primers were concatenated with universal hybrid tails (T7 Promoter for forward and T3 for reverse primers). The universal tails are shown in bold.

Table S2. List of exemplars and sequences used in the study along with Genbank along with accession numbers. Newly added sequences are presented in bold. A hyphen indicates that no sequence is available.

Table S3. Partition schemes and best-fit models of sequence evolution used to reconstruct the phylogeny of Uropeltis under the MrBayes and BEAST analyses. Codon position is represented by cp1, cp2 and cp3.

Table S4. Fossil calibrations used for the divergence dating analysis of uropeltid snakes in BEAST.

Table S5. Results of interclass correlation coefficient (ICC) calculation using a single-rating, absolute-agreement, two-way random-effects model. ICC is a measure of the strength of inter-rater agreement between different groups, and ranges from 0 to 1. Values close to 0 indicates dissimilar scores within each species, while a value close to 1 indicates highly similar scores within the same species. ICC was calculated using the 'irr' v.0.84.1 package (Gamer *et al.*, 2019) in R v.3.5.2 (R Core Team, 2016).

Table S6. Description of morphometric measurements collected from specimens of *Uropeltis* species.

Table S7. Phylogenetic signal of each of the morphological variable for *Uropeltis* species using Pagel's lambda (λ), Blomberg's K and a multivariate estimate of phylogenetic signal (K_{mult}). The phylogenetic signal for the multivariate data (K_{mult}) was estimated using the *physignal* function in the geomorph v.3.0.7 package. Values in bold indicate statistically significant values.

Table S8. Loading of morphological variables from the phylogenetic principal component analysis (pPCA). The pPCA was performed after size correction of morphological variables using phylogenetic regression of each trait with SVL. Bold values indicate strong loading (> 0.60).

Table S9. Summary and comparison of different models fit using the pPCA of morphological variables as explanatory variables and the overall conspicuousness score (ΣCS_i) as response variable in *Uropeltis* species based on a phylogenetic generalized least square (PGLS) regression. Model in bold indicates the best-fit model. '*' indicates variables that are statistically significant ($P < 0.05$).

Table S10. Comparison of the fit of different models of trait evolution for the three principal components obtained from the morphometric measurements of *Uropeltis* species under the three threshold conspicuous schemes. The best-fit model under each of the three schemes is indicated in bold.

Table S11. Loading of head-shape variables of *Uropeltis* snakes from a phylogenetic principal component analysis (pPCA). The pPCA was performed after size correction of head shape variables using phylogenetic regression of each trait with SVL. Bold values are strong loading (> 0.60).

Table S12. Comparison of the fit of different models of trait evolution for the three principle components obtained from only the head measurements of *Uropeltis* species under the three threshold conspicuous schemes. The best-fit model under each of the three schemes is indicated in bold.

Figure S1. Representative images of the dorsal and ventral colouration of *Uropeltis madurensis*: alive (A, dorsal; B, ventral) and after preservation (C, dorsal; D, ventral). Note that the yellow dorsal and ventral colouration are discoloured in the preserved specimens (C and D) but can be differentiated from the background black colouration.

Figure S2. Bayesian phylogeny (50% majority rule tree) of Uropeltis from the MrBayes analysis. Node values indicate posterior probabilities.

Figure S3. Representative images of the ventral colouration of *Uropeltis* species used in this study. A, *U. liura*; B, *U.* cf. *ochracea*; C, *U. nitida*; D, *U.* cf. *beddomii*; E, *U. bhupathyi* (Image: Jins V.J.); F, *U. pulneyensis*; G, *U. maculata*; H, *U.* cf. *ellioti* (Mysore); I, *U.* cf. *ellioti* (EG); J, *U.* cf. *ceylanicus* (PMB); K, *Uropeltis sp.* (Ponmudi); L, *U.* cf. *ceylanicus* (Kannur); M, *U.* cf. *arcticeps* (Elepara); N, *U.* cf. *ceylanicus* (Athirapalli); O, *U.* cf. *myhendrae* (Image: Umesh P.K.); P, *Uropeltis sp.* (Munnar); Q, *U. madurensis*; R, *U. myhendrae*; S, *U.* cf. *ellioti* (TN); T, *U.* cf. *phypsoni* (Wayanad); U, *U.* cf. *nilgherriensis* (Wayanad); V, *U.* cf. *m. macrolepis*; W, *U.* cf. *m. mahabaleshwarensis*; X, *U.* cf. *phipsoni* (Pune).